Earthquakes and Structures, *Vol. 5, No. 3(2013) 277-296*
DOI: http://dx.doi.org/10.12989/eas.2013.5.3.277

Seismic progressive collapse assessment of 3-story RC moment resisting buildings with different levels of eccentricity in plan

Somayyeh Karimiyan[a], Abdolreza S. Moghadam[*] and Mohammad G. Vetr[b]

Int'l Institute of Earthquake Eng. and Seismology (IIEES), No. 21, Arghavan St., North Dibajee, Farmanieh, Tehran, Iran

(Received April 10, 2013, Revised May 22, 2013, Accepted June 10, 2013)

Abstract. Margin of safety against potential of progressive collapse is among important features of a structural system. Often eccentricity in plan of a building causes concentration of damage, thus adversely affects its progressive collapse safety margin. In this paper the progressive collapse of symmetric and asymmetric 3-story reinforced concrete ordinary moment resisting frame buildings subjected to the earthquake ground motions are studied. The asymmetric buildings have 5%, 15% and 25% mass eccentricity. The distribution of the damage and spread of the collapse is investigated using nonlinear time history analyses. Results show that potential of the progressive collapse at both stiff and flexible edges of the buildings increases with increase in the level of asymmetry in buildings. It is also demonstrated that "drift" as a more easily available global response parameter is a good measure of the potential of progressive collapse rather than much difficult-to-calculate local response parameter of "number of collapse plastic hinges".

Keywords: asymmetric buildings; progressive collapse; mass eccentricity; reinforced concrete ordinary moment resisting frame building; nonlinear time history analysis; flexible edge; stiff edge

1. Introduction

The progressive collapse of a structure is initiated by propagation of local damages which lead to collapse of a major portion of the structure, in such a way that the structural system cannot bear the gravity and lateral structural loads. In this process, the final damage state is much more than the initial damages Ellingwood (2006). There are a number of abnormal loads which can potentially be the trigger of progressive collapse such as aircraft impact, fire, accidental overload, design/construction error, gas explosions, bomb explosions, hazardous materials, vehicular collision, etc (Somes 1973, Burnett 1975a).

Computationally macro models have developed to compare progressive collapse in 2 dimensional ten-story steel moment resisting frames, seismically designed for high and moderate

[a] Ph.D. Candidate, E-mail:s.karimiyan@iiees.ac.ir
[*]Corresponding author, Assistant professor, E-mail: moghadam@ iiees.ac.ir
[b] Assistant professor, E-mail: vetr@ iiees.ac.ir

 ISSN: 2092-7614 (Print), 2092-7622 (Online)

seismic risks, based on current design specifications with usage of beam and column finite-element models. Results of the simulation showed that the progressive collapse potential in the frames, designed for high seismic, is less than the moderate seismic risk. To have a better resistance to progressive collapse, system strength is more effective than the improved ductile detailing in the structural systems and also the alternate path method was demonstrated as a useful method against the progressive collapse potential (Khandelwal *et al*. 2012).

This macro model-based simulation was also used in 2-dimensional RC moment frames designed for lateral load requirements in seismic and non seismic regions. Results illustrated that designing based on the high seismicity zone provisions and using special RC moment frame in buildings are more effective than RC frame structures designed for low or moderate seismic risk in progressive collapse evaluation. Using a macro model-based approach is viable to investigate progressive collapse mechanism (Bao *et al*. 2012).

Collapse mechanisms and earthquake resistance to progressive collapse were investigated by Gurley (2012) via comparing sway collapse mechanisms in earthquake engineering and double-span mechanisms of GSA (2003) under explosion loads (removal columns). Based on the results, since earthquake damages can also remove the load bearing elements similar to the explosion loads, assessment of progressive collapse in the presence of earthquake loads is vital for designing against the progressive collapse. Investigation of the ductile detailing and ductile detailing for the lost column events relevant to the specific collapse mechanisms showed that design according to earthquake engineering is a valuable method for designing against progressive collapse and it needs to include the "double span" mechanisms at lost columns.

One of the most frequently used procedures for resistance to progressive collapse has shown the alternate path method. Evaluation of the overall stability of moment-resisting (sway) frames and nonsway frames which include lateral-force resisting elements showed that considering the global response of the damaged structures are necessary for assessment of progressive collapse and also demonstrated that the progressive collapse investigations should be applied to seismic and direct blast hazards (Ettouney *et al.* 2012).

Progressive collapse mechanism of RC frame structures were studied with assessment of two typical non-integrated slab and integrated cast-in-situ slab with different levels of seismic fortification (Yi *et al*. 2011). Then the alternate path (AP) method was evaluated by investigation of the results of nonlinear dynamic analyses.

Contribution of framed beams resisting to progressive collapse resulted by the initial damages in various locations showed that the inadequacy of lateral stiffness of the columns leads to the distribution of collapse in horizontal directions. Assessment of the slabs effects and seismic design levels demonstrated that the catenary action provides resistance to progressive collapse mechanism in the continuous beams whit sufficient horizontal constraint at both ends.

The relationship between progressive collapse and earthquake-resistant RC buildings were studied by Tsai and Lin (2008) according to GSA guidelines. Linear static, nonlinear static and nonlinear dynamic analyses were performed in the structures subjected to the columns removal. Results showed that because of the different collapse resistances, GSA criteria should be different for the two different nonlinear analyses and a dynamic amplification factor (DAF) of 2 causes the nonlinear static method to be conservative. Also it is required to consider DAF in the inelastic dynamic effects in GSA linear procedure. Nonlinear static capacity curve showed that it is possible to predict DAF and progressive collapse resistance in the column-removed RC buildings (Tsai and Lin 2008).

The progressive collapse simulation of 12-story, 3-bay precast panel shear wall in the presence of earthquakes loads were investigated by Pekau and Cui (2005) through a distinct element method (DEM) program. Integrity analyses were performed and shear ductility demands of the mechanical connectors in the vertical joints were investigated. Simulation of the progressive collapse processes of the panel wall in various conditions illustrated that if precast panel shear wall satisfies the seismic requirements, it will automatically provide the demands of shear ductility of connectors in vertical joints and shear slip in horizontal joints in progressive collapse assessment.

Three databases on experimental data of reinforced concrete beams, steel W-beams and tubular hollow square steel columns were developed to simulate the dynamic response until the collapse of the buildings. These databases were used to quantify important parameters which affect the cyclic moment-rotation relationship at plastic hinge regions in the steel and RC components subject to the earthquake loads. The application of these databases in the field of performance-based earthquake engineering has been illustrated via a study of a 4-story steel structure. Results showed that its seismic performance was successfully assessed in collapse evaluation of the building (Lignos and Krawinkler 2012).

Eslami and Ronagh (2012) used lumped plasticity method in RC members to compare the plastic hinges which are defined based on the properties of RC members and those of defined according to the FEMA-356 by pushover analysis. They determined accurately the force–deformation curves of the defined hinge, via considering the material inelastic behavior, dimensions of the members and reinforcement details. An eight-story and two four-story frames were investigated with various ductilities. Results of the hinging pattern, inter-story drift, the pushover curve and the failure mechanism showed that FEMA-356 hinges underestimate the strength and the displacement capacity, particularly for the frame with low ductility.

Based on the databank of experimental tests in reinforced concrete members, a number of models were developed to calculate the moment-rotation, ultimate deformation in beams and columns and the secant stiffness at flexural yielding. These models present the explicit and simple expressions which are proper for the practical applications, without any dependency to analyze the moment-curvature. Then, the effects of biaxial loading on member yielding and ultimate deformation are investigated. Results showed that the proposed models are suitable and valuable for the seismic evaluation and retrofitting of the reinforced concrete buildings (Biskinis and Fardis 2009).

More than 1000 experimental tests were done by Panagiotakos and Fardis (2009) on RC beams and columns to develop formulas to determine deformations of the reinforced concrete members at yielding or failure according to the geometric and mechanical properties of the members. Yield and ultimate curvature formulations provide good average agreement with the experimental test results, but with a large scatter. The same procedure was repeated for the ultimate drift or chord-rotation capacity according to the curvatures and the concept of plastic hinge length. Semi-empirical models for the drift or chord-rotation at member yielding provide good average agreement with the test results, but with a considerable scatter. Their estimation in the effective elastic stiffness of the cracked reinforced concrete buildings has 20% scatter in comparison with the test results.

One of the most frequently used approaches to investigate the results of nonlinear static and dynamic analyses is to use concentrated plasticity models which are available in many softwares. Dides and Liera (2005) evaluated three different concentrated plasticity models in the presence of the earthquake loads and compare their limitations and priorities. Namely, 1) a simplified macro element model in a complete building story, 2) elasto-plastic interaction hinges and 3) fiber hinges.

These models are investigated in a 1-story steel asymmetric plan building and also in a 3-story steel building. Results showed that in the simplified macro element model the global responses are obtained with average deviation of 20% in comparison with those of the other two concentrated plasticity models.

An improved spread plasticity model was proposed by Kyakula and Wilkinson (2004) to identify the initiation point of yielding throughout the beams. The model considers the gradual spread of plasticity, actual length of the yield zones and also can shift the points of contra flexure through the beams with assuming that columns and beam-column joints remain elastic. Some examples were used to investigate the limitations of the existing spread plasticity models. Results show that the existing spread plasticity models which consider plasticity just at beam and column connections are accurate for the lower stories and structures where the gravity loads are smaller than the seismic loads. Comparing the results of the proposed and existing spread plasticity models on various examples demonstrated that their proposed model improves the accuracy of the global displacements, inter story drift ratios and joint rotations up to 25%.

Most of research works in the context of progressive collapse have studied column removal under explosion loads or collisions. (Helmy *et al*. 2012, Hayes Jr *et al*. 2012, Masoero *et al*. 2010, Khandelwala *et al*. 2009, Talaat and Mosalam 2009, Sasani and Kropelnicki 2008, Sasani and Sagiroglu 2008, Sasani and Sagiroglu 2008, Sasani *et al*. 2007, El-Tawil *et al*. 2007, Bažant and Verdure 2007, Lew 2003, Kaewkulchai and Williamson 2003).

However, there are a few researches that have considered the 3D progressive collapse of the buildings under earthquake loads and torsion effects. In 2011, rotational friction dampers were investigated against the earthquake loads and progressive collapse resisting capacities (Kim *et al*. 2011).

Progressive collapse numerical simulation in reinforced concrete (RC) frames and RC shear-walls subjected to the earthquake loads were done using multi-layer-shell-element and fiber-beam-element models (Lu *et al*. 2008). Nonlinear behavior of RC structural elements were simulated including the cyclic behavior under coupled axial force-bending moment and shear force, breakdown of the structural elements at ultimate states and contact between the structural elements during the collapse (Lu *et al*. 2008).

Planar models in comparisons with the 3D models were studied in 2011 with different assumptions in model simulations (Alashker *et al*. 2011). A few 10-story steel buildings, seismically designed in planar and 3D macro models, were considered to investigate the 2D and full 3D structural systems due to forcibly columns removal. Four different types of models were used to examine the various simulation approaches in progressive collapse assessments. Results showed that floor systems have significant effects on the distribution of the collapse response in 3D macro models. Therefore, because of the floor system contribution effects, 3D models were conservative and valuable in progressive collapse evaluation in comparisons with the planar models.

Progressive collapse mechanism in symmetric and asymmetric buildings was evaluated as a result of columns removal through designing 30-story regular and irregular structural models once with braced cores and once more with reinforced concrete cores. The results of analyzing the irregular structural models have shown that variation of the progressive collapse resisting capacities, were based on the location of removed columns. Progressive collapse potential of the irregular structure was increased, when the location of the removed column was determined in the tilted side of the building. The plastic hinges formed in the removed column bays and adjacent bays showed that other elements in the structural system were involved in resisting progressive

collapse and when a structural member was removed, other elements contributed to resist against the progressive collapse. So, progressive collapse potentials of the asymmetric buildings were not very large in comparison with those of the corresponding symmetric buildings (Kim and Hong 2011).

Although there are many cases of the collapsed buildings in past earthquake events, usually the spread of collapse is not considered explicitly in seismic design or evaluation of the buildings. In this research the spread of collapse in the building subjected to the earthquake ground motion records is studied by continuing nonlinear time history analyses even if some elements pass their collapse limit state.

Past earthquakes have shown that torsion in asymmetric plan buildings usually causes concentration of damage in one side of those buildings. Therefore it is expected that asymmetry in a building increases the progressive collapse potential of the building.

In the present study, to evaluate the effect of asymmetry on the seismic progressive collapse potential of low rise buildings, a set of regular and irregular 3-story ordinary moment resisting frame RC buildings are considered. At first, a regular building is designed based on ACI (2005), and then by introducing mass eccentricities of 0.05, 0.15, and 0.25 in the symmetric structural model, asymmetric version of the model buildings are created. Then, they are analyzed using a set of 2-component earthquake ground motion records.

Three-story buildings have been chosen to consider the extensive range of the common office, commercial and residential buildings in most countries. Via such a study, we can present valuable criteria to investigate progressive collapse potential of the low rise buildings including 3-story buildings.

There are many weak and traditional buildings in most countries. On the other hand, as we addressed in the paper, the aim of this study is to investigate potential of the progressive collapse in the structures. The probability of collapse occurrence in a building designed with ordinary moment resisting frames is higher than those with special or moderate moment resisting frames. For this reason, we believe that the building models with ordinary moment resisting frame are more important to be evaluated in terms of potential of the progressive collapse in comparison with the other building types.

The level of 25 percent mass eccentricity is considered to include the extreme amount of irregularity in the buildings. Moreover, we consider such an extreme amount of irregularity, because there are a few special structures in common buildings that have a mass eccentricity level more than 25%.

2. The reference building

The basic model is a regular 3-story reinforced concrete ordinary moment resisting frame building (Fig. 1(a)). This is a 3-bay by 3-bay building that each bay has a span of 5m center to center. The story height of all stories is 3.5m. The design dead load is 5.3 KN/m^2 and the design live load is 1.96 KN/m^2. The design base shear factor of the building is 0.2159. Building is designed as ordinary moment resisting frame system based on ASCE (2010).

It is worth mentioning that the effects of infills are not considered in our study.

The asymmetric building models are derived from the basic model by changing their mass distribution. The mass distribution is determined to produce equal one way mass eccentricity in all floors in the x-direction. A total of four building models with eccentricities equal to 0, 5, 15 and 25

percent are considered in this study.

Mass has been concentrated in the nodes of the frames according to its mass tributary area in the building models. The mass in each floor is distributed equally among the frame nodes in a symmetric building. Fig. 1(b) shows the typical mass distribution in the symmetric building. In asymmetric buildings mass has been distributed in nodes of the frames in such a way that the value of lumped mass for the two left side frames are more than those in two right side frames.

It is worth to mention that two conditions were considered in the mass distribution:

- The summation of mass values in asymmetric buildings is equal to the symmetric one.
- The distance of mass center from the center of rigidity provides the required mass eccentricity.

As an example Fig. 1(c) shows the mass distribution in building with mass eccentricity of 15%.

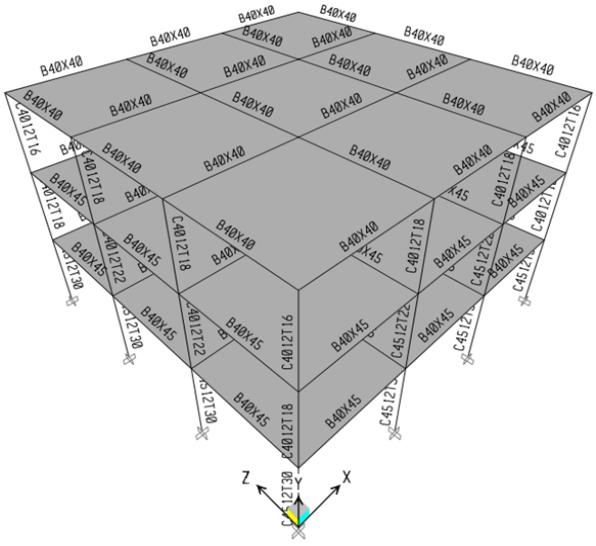

(a)

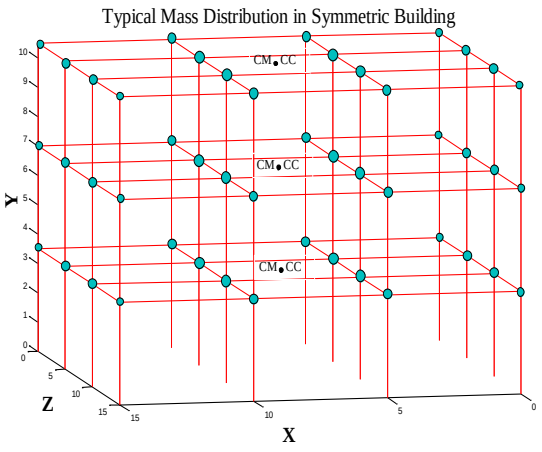

(b)

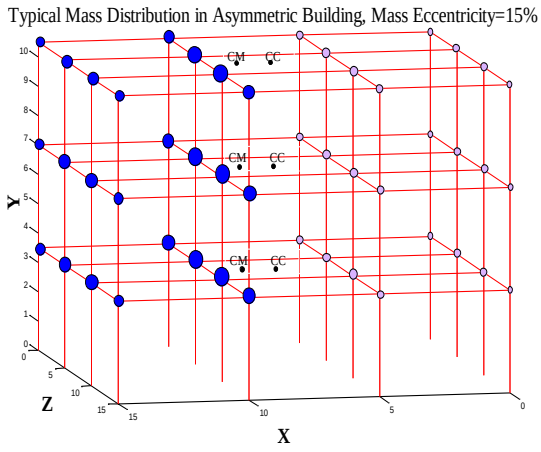

(c)

Fig. 1 (a) View of the building model, (b) Typical mass distribution in a symmetric building and (c) Typical mass distribution in an asymmetric building

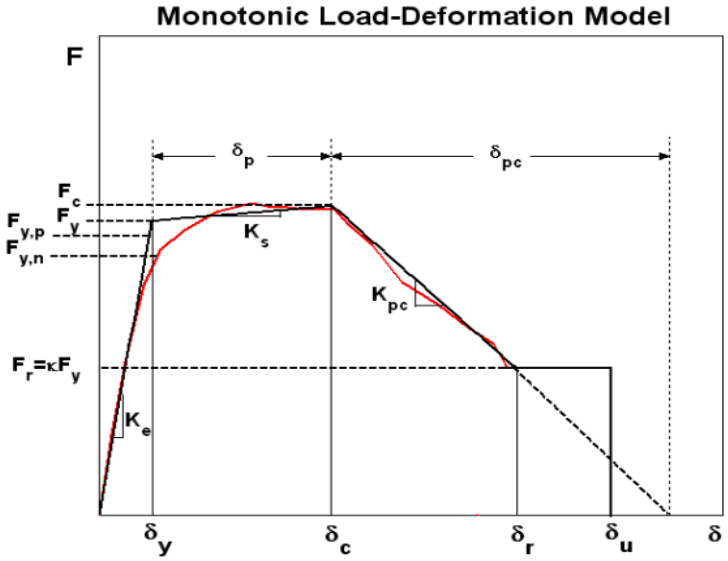

Fig. 2 Backbone curve of modified Ibarra-Krawinkler model and its associated definitions (Ibarra *et al*. 2004 and 2005, Lignos 2008, Lignos *et al*. 2008, Krawinkler *et al*. 2009, Haselton *et al*. 2009)

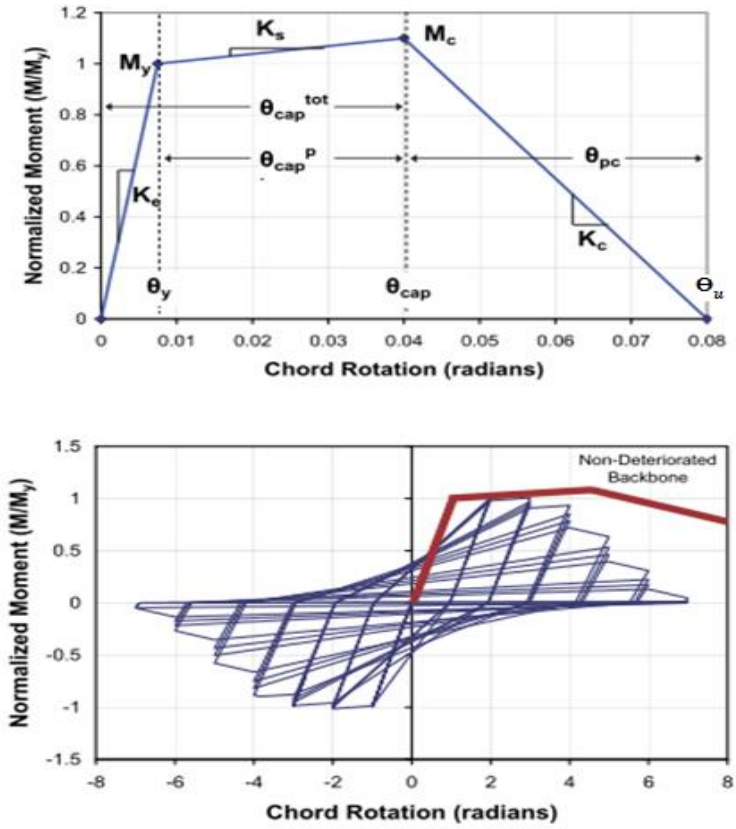

Fig.3 Monotonic and cyclic behavior of component model used in this study (Ibarra and Krawinkler 2005, Haselton *et al*. 2007 and 2008, FEMA P695 2009, Zareian *et al*. 2009 and 2010)

All records have two components which are applied on the structures in two horizontal directions X and Z in such a way that the Z components are stronger than X components in all earthquake records.

Even though many reinforced concrete element models exist, most of them cannot be used to simulate structural collapse (FEMA P695 2009).

It has been shown that the careful selection of the element backbone curves is essential for a proper simulation of the collapse in buildings FEMA P695 (2009). In this study, the calibrated beam-column element model which is led to the global collapse of RC frame buildings is the one developed by Ibarra, Medina and Krawinkler (2005). Fig. 2 shows the backbone curve of the modified Ibarra-Krawinkler model, and its associated definitions (for more details on the notations used in Fig. 2, the reader may refer to the Appendix). This model includes such main aspects as the "capping point", where monotonic strength loss begins, and the post-capping negative stiffness. These features enable modeling of the strain-softening behavior associated with concrete crushing, rebar buckling and fracture, or bond failure FEMA P695 (2009).

In general, accurate simulation of the side-sway structural collapse depends on the proper modeling of the post-capping behavior. Researchers have also used a variety of other methods to simulate cyclic response of reinforced concrete beam-columns, including the fiber models that can capture cracking behavior and the spread of plasticity throughout the element Filippou (1999). The decision of using a lumped-plasticity approach is based on this observation that the currently available fiber elements models are not capable of simulating the strain-softening associated with rebar buckling, and thus, cannot reliably simulate the collapse of flexural dominated reinforced concrete frames.

Also, currently available steel material models are not able to replicate the behavior of rebar as it buckles and fractures. Due to this limitation, current fiber models were judged inadequate for simulating collapse in RC and steel buildings. Research is ongoing, and this modeling limitation may be overcome in the near future.(Ibarra and Krawinkler 2005, Haselton *et al.* 2007, FEMA P695 2009).

In this paper, the nonlinear behavior is represented using the concentrated plasticity concept with rotational springs. The rotational behavior of the plastic regions in models is according to the Modified Ibarra, Medina and Krawinkler Deterioration Model (Ibarra *et al.* 2005, Lignos and Krawinkler 2012).

The input parameters for the rotational behavior of the plastic hinges in models are determined using empirical relationships developed by Lignos and Krawinkler (2012) which have been derived from an extensive database of RC component tests. Alternately, these input parameters can be determined using approaches similar to those described in FEMA P 695 and Haselton and Deierlein (2007).

So, the zero length spring elements are connected to the both ends of elastic beam and column elements. In other words, moment resisting frames are modeled with elastic beam-column elements connected by zero length elements which serve as rotational springs to represent the structure's nonlinear behavior. As mentioned before, the springs follow a hysteretic response based on the Modified Ibarra, Medina and Krawinkler deterioration model. The effect of the plastic hinge length is considered in calculation of rotational behavior of the plastic hinges empirically from the test data (Haselton *et al.* 2007, FEMA P695 2009, Lignos and Krawinkler 2012, Panagiotakos and Fardis 2009, Biskinis and Fardis 2009).

It is worth mentioning that, the effect of the concrete strength is considered in this study to calculate the parameters which are related to the modified Ibarra-Krawinkler model (which is used

to identify nonlinear behavior of the elements). But its value is constant in all symmetric and asymmetric building models. In other words, the effect of changing the concrete strength is not investigated in this research. As we used the common concrete design codes and their seismic regulations, the range of concrete strength which is permitted in design, is such that the effect of the brittle behavior is not expected. The Fc parameter which is considered in this study is equal to a constant value of 28 MPa for all symmetric and asymmetric building models.

According to Fig. 2, to simulate the structural collapse, parameter κ should be zero. Also, based on the modified Ibarra-Krawinkler model shown in Fig. 3, zero strength corresponds to Θu. It means that as soon as value of Θ reaches to Θu, hinge strength would be equal to zero, meaning the element is effectively eliminated from the structure. In other words, during nonlinear time history analysis, when the value of Θ for a hinge reaches to its corresponding Θu value, the relevant beam or column element would be removed from the structural system automatically and nonlinear time history analysis continues till the analysis is completed or the structural system

Table 1 Summary of the used PEER NGA Database information and Parameters of Recorded Ground Motions for the Far-Field Record Set FEMA P695 (2009)

ID No.	PEER-NGA record information				Recorded Motions	
	Records Seq. No.	Lowest Freq (Hz.)	File names – Horizontal record		*PGA max* (g)	*PGV max* (cm/s.)
			Component 1	Component 2		
1	953	0.25	NORTHR/MUL009	NORTHR/MUL279	0.52	63
2	960	0.13	NORTHR/LOS000	NORTHR/LOS270	0.48	45
3	1602	0.06	DUZCE/BOL000	DUZCE/BOL090	0.82	62
4	1787	0.04	HECTOR/HEC000	HECTOR/HEC090	0.34	42
5	169	0.06	IMPVALL/H-DLT262	IMPVALL/H-DLT352	0.35	33
6	174	0.25	IMPVALL/H-E11140	IMPVALL/H-E11230	0.38	42
7	1111	0.13	KOBE/NIS000	KOBE/NIS090	0.51	37
8	1116	0.13	KOBE/SHI000	KOBE/SHI090	0.24	38
9	1158	0.24	KOCAELI/DZC180	KOCAELI/DZC270	0.36	59
10	1148	0.09	KOCAELI/ARC000	KOCAELI/ARC090	0.22	40
11	900	0.07	LANDERS/YER270	LANDERS/YER360	0.24	52
12	848	0.13	LANDERS/CLW-LN	LANDERS/CLW-TR	0.42	42
13	752	0.13	LOMAP/CAP000	LOMAP/CAP090	0.53	35
14	767	0.13	LOMAP/G03000	LOMAP/G03090	0.56	45
15	1633	0.13	MANJIL/ABBAR--L	MANJIL/ABBAR—T	0.51	54
16	721	0.13	SUPERST/B-ICC000	SUPERST/B-ICC090	0.36	46
17	725	0.25	SUPERST/B-POE270	SUPERST/B-POE360	0.45	36
18	829	0.07	CAPEMEND/RIO270	CAPEMEND/RIO360	0.55	44
19	1244	0.05	CHICHI/CHY101-E	CHICHI/CHY101-N	0.44	115
20	1485	0.05	CHICHI/TCU045-E	CHICHI/TCU045-N	0.51	39
21	68	0.25	SFERN/PEL090	SFERN/PEL180	0.21	19
22	125	0.13	FRIULI/A-TMZ000	FRIULI/A-TMZ270	0.35	31

becomes unstable. In this study a hinge is considered as collapsed one if its rotation exceeds the extreme value of Θu.

The nonlinear dynamic time history analyses are performed here using OPENSEES (Version 2.2.2) software, employing 2-component ground motion records according to the FEMA P695, Table A-4C, as shown in Table 1. Only two hinges have been considered at both ends of all beams and columns in OPENSEES structural model.

Each record is normalized to the different PGA levels of 1g to 3g. These PGA levels are used to exert the intensive effect of the earthquake intensity on the structure elements, causing the collapse of the beams and columns one after another and consequently, the collapse probability increases in the whole structure FEMA P695 (2009).

For example, Fig. 4 demonstrates the progressive collapse of an irregular building with mass asymmetry of 25% for the earthquake record #848 from the collapse of the first hinge to the collapse of a large portion of the structure.

The numbers in Fig. 4 show the sequence of the collapsed hinges which formed in the building from the first hinge to the 54th hinges (the building becomes unstable after the formation of 54 hinges). However, the first 20 collapsed hinges are shown with different colors in such a way that the darker colors demonstrate those hinges which are collapsed in the earlier stage of NLTHA. The light colors also demonstrate the hinges which are collapsed in the final step of the NLTHA. In

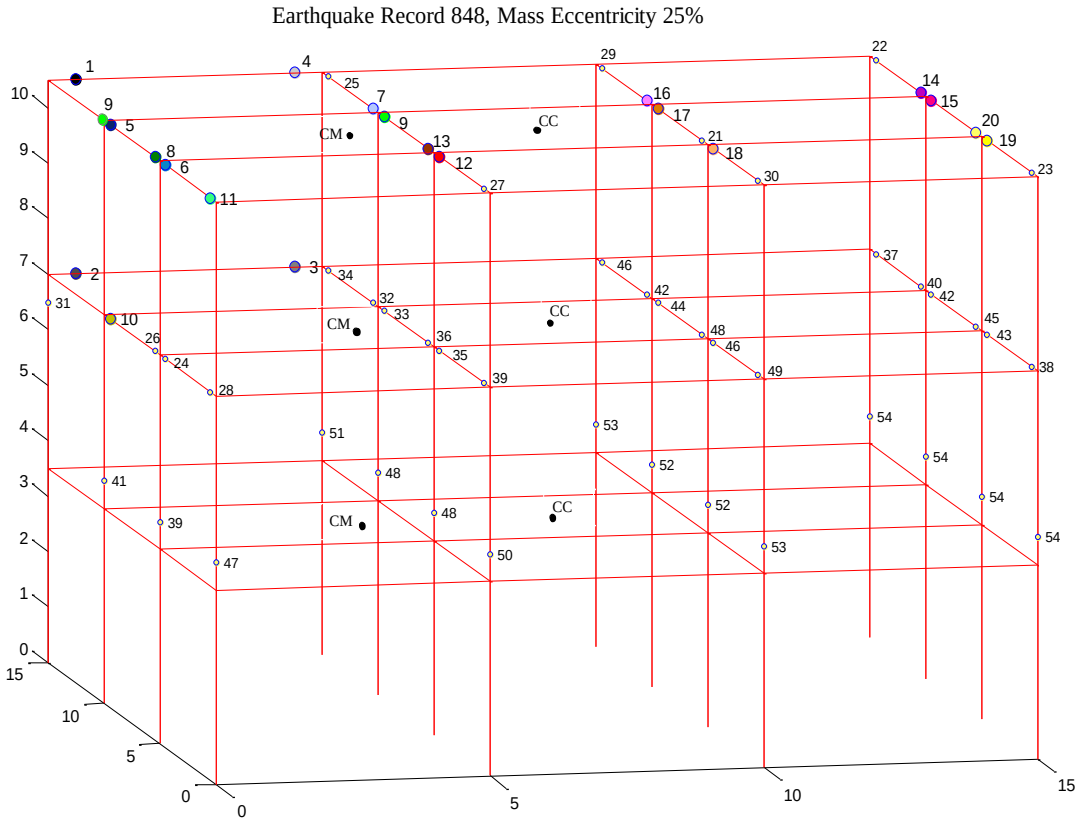

Fig. 4 Progressive collapse in an asymmetric building with mass eccentricity of the 25 percent in presence of the earthquake record #848

other words, the sequence of collapsed hinges has been illustrated from the first hinge to the last hinge with a coloring rational which goes from dark to light. Although the numbers demonstrate the sequence of collapsed hinges, but using the colors is useful to get a rapid visual sense of the trend of collapse in the building. As an example in Fig. 4, the hinge which is tagged as the #1 and is colored black is the first collapsed hinge which is formed in the left side of the beam which is in the back frame of the third floor during NLTHA. In this way, the first point in the structure which starts to collapse and subsequently will be eliminated from the load bearing structural system is determined. Then, NLTHA continues till the second point in the building being collapsed and eliminates from the load bearing structural system (such a collapsed hinge is tagged as #2 and is colored dark blue in the left side of the back frame beam in the second floor).

In this way, the 3th, 4th to 54th collapsed hinges are shown one after another with both the numbers and colors. Consequently, the probability of the collapse is larger in the formed hinges with lower numbers and darker colors. In this way, the sequence of collapsed hinges which are formed one after another in the beam and column elements of the regular and irregular buildings are identified. This process is repeated for other earthquake records in symmetric and asymmetric buildings with various mass eccentricities, too.

The response spectra of the both components of each record are shown in Fig. 5(a) and 5(b).

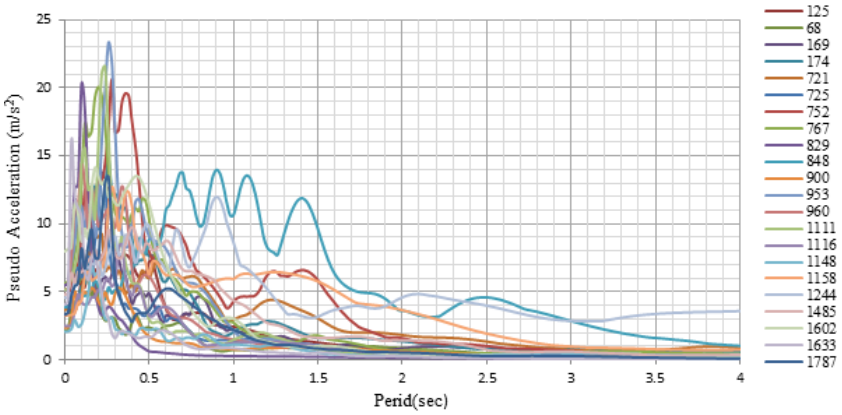

(a) Z Components

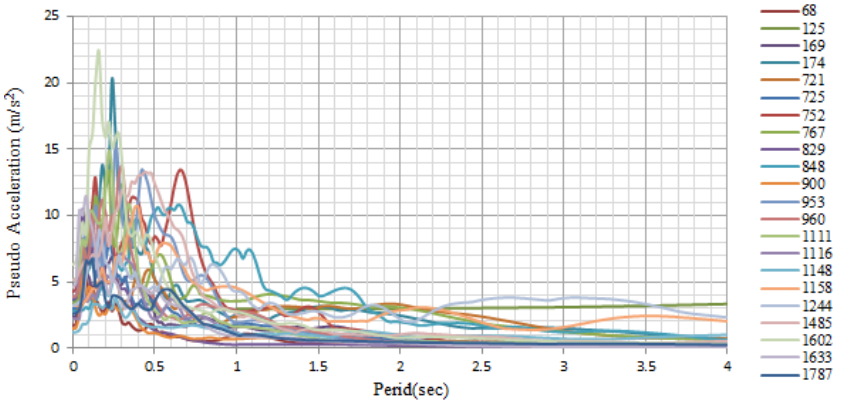

(b) X Components

Fig. 5 Pseudo acceleration spectrum of ground motion records: (a) Z Components and (b) X Components

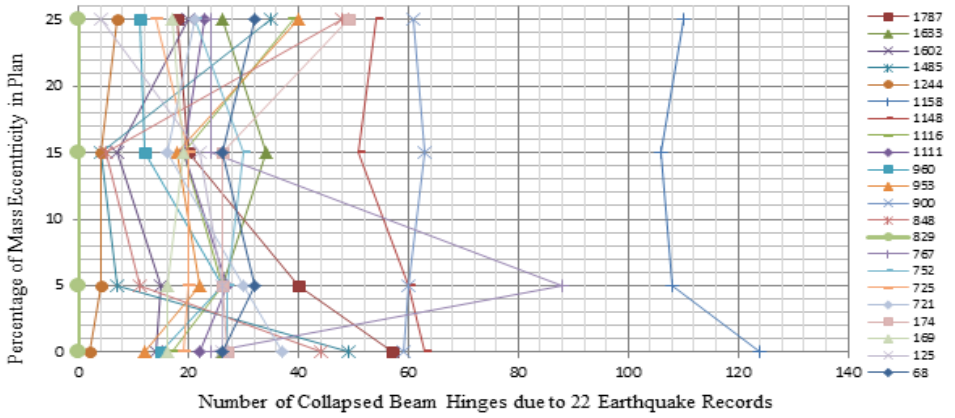

(a)

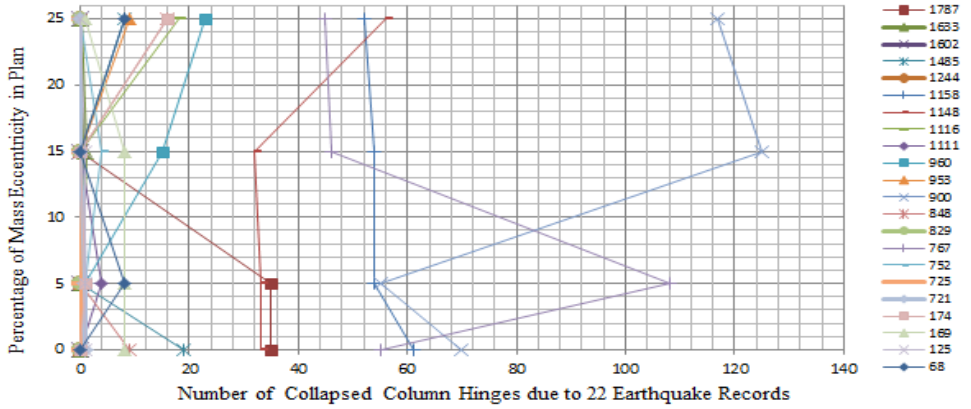

(b)

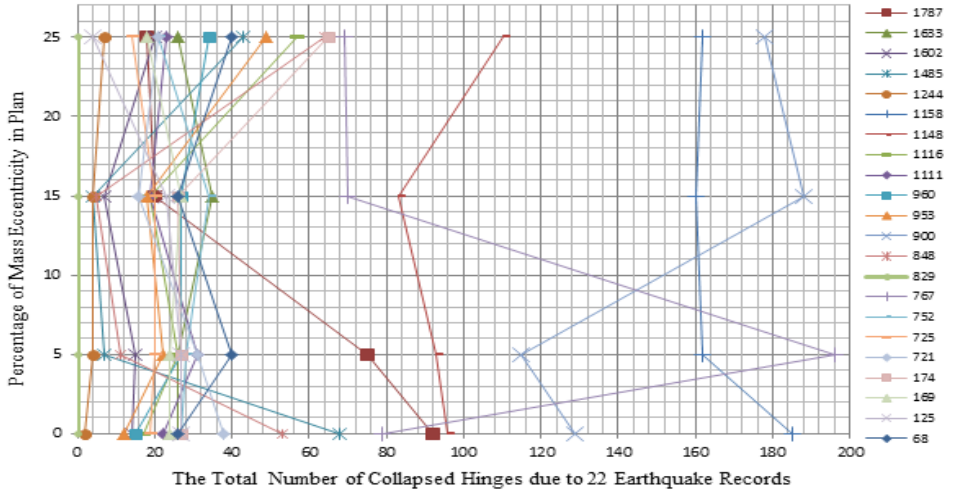

(c)

Fig. 6 Number of collapsed hinges due to 22 ground motion records in building models with 0%, 5%, 5% and 25% mass eccentricities; a: number of hinges in beams, b: number of hinges in columns, and c: total number of hinges

Table 2 The first five periods of the buildings structural models (sec)

Mass Eccentricity in Floors	T1	T2	T3	T4	T5
%0	0.788	0.779	0.672	0.24	0.237
%5	0.785	0.781	0.654	0.243	0.238
%15	0.869	0.782	0.576	0.261	0.239
%25	0.909	0.781	0.479	0.277	0.239

Fig. 6(a), 6(b), and 6(c) show the number of collapsed beam and column hinges for each of 22 ground motion records in building models with 0%, 5%, 15% and 25% of mass eccentricities. The number of collapsed hinges in beams and columns are shown in Fig. 6(a) and 6(b), respectively, and the total number of collapsed hinges is shown in Fig. 6(c).

According to Fig. 6, the number of collapsed hinges in records #1158, 1148, 767 and 900, in different mass eccentricities, are more than the other records. A comparison of building periods in Table 2 with those of ground motion response spectra in Fig. 5 identifies that these records are the cases with high spectral acceleration values in their main periods. This is a reason to observe that when mass eccentricity increases, there is no further increment in the number of collapsed hinges in these ground motion records.

To find the relation between the number of collapsed hinges and the amount of increment in mass eccentricity, the number of collapsed hinges in the buildings with various mass eccentricities of 0, 5, 15 and 25 percent are compared with each other for each earthquake ground motion. Then, the percentages of increase in the number of collapsed hinges are calculated in the entire buildings. Fig. 7 shows the percentage of increase in the number of collapsed hinges as the mass eccentricity increases in plan in the presence of 22 earthquake records.

As said before, the most important purpose of this paper is to investigate the increase or decrease steps of the number of the collapsed hinges when the building eccentricity goes from one level to another level.

To calculate the percentages of increase in the number of collapsed hinges which are shown in Fig. 7, two cases of the earthquake recodes # 1787 and # 1116 are explained as follows; according to Figure 6c, for the earthquake record #1787, the number of collapsed hinges in the buildings with mass eccentricity of 0, 5, 15 and 25 percent is 92, 75, 20 and 18, respectively. There are three decreasing steps as follows:

92 75 20 18

Decreasing step Decreasing step Decreasing step

The percentage portion of each decreasing steps is 33.33%. It should be noted that summation of three decreasing steps in this case equals to 100%. Since all steps are decreasing, and there is no increasing steps from one level of mass eccentricity to the other one, decreasing in the number of collapsed hinges is 100% which is equivalent to say that increasing in the number of collapsed hinges is equal to 0% for record # 1787 as shown in Fig. 7.

In a similar way, according to Fig. 6(c), the number of collapsed hinges in buildings with mass eccentricity of 0, 5, 15 and 25 percent are 17, 26, 19 and 57, respectively for the earthquake record # 1116. Based on the data, two increment steps from 0 to 5% and 15 to 25% and a reduction step

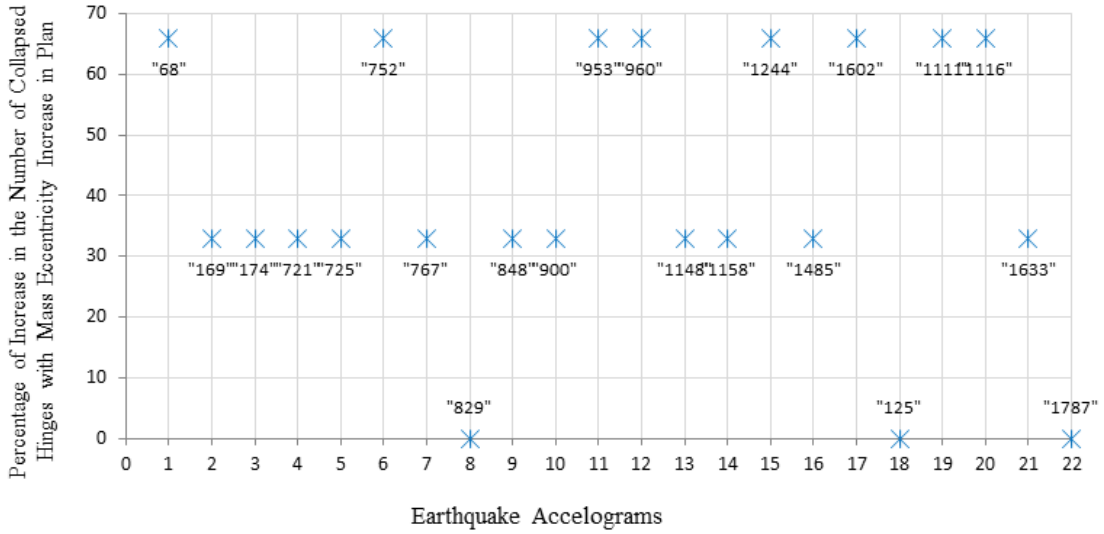

Fig. 7 The percentage of increase in the number of collapsed hinges with the mass eccentricity increase in plan

from 5 to 15% are observed in the number of collapsed hinges.

17 26 19 57

Increasing step Decreasing step Increasing step

Since, 2 out of 3 (i.e. 66.67%) steps are increasing, we say that the percentage of increase in the number of collapsed hinges as the mass eccentricity increases from 0 to 25% is equal to 66.67% (a 33.33% for increment step from 0% to 5% and another 33.33% for increment step from 15% to 25%).

The same procedure is repeated for the other earthquake records. Results show that the number of collapsed hinges or in the other words, the potential of progressive collapse, increases when the mass eccentricity increases in the buildings plan.

Drift and displacement are among the usual acceptance criteria in building codes. In this part, the relation between drift and the number of collapsed hinges is investigated. Driving such a relationship can highly simplify the sidesway collapse investigation of moment resisting frame buildings. To compare the structural behavior of the symmetric and asymmetric buildings, story drifts are derived for various mass eccentricities in different edges of the buildings. The closer and the farther edges to the mass center are defined here as flexible and stiff edges respectively.

The percentage of increase in the story drifts in mass centers, stiff and flexible edges with increasing the mass eccentricity of the building models are shown in Fig. 8 separately, and their average are shown in Fig. 9.

To calculate the percentages of increase in the story drifts in mass centers, stiff and flexible edges resulted by increasing the degree of asymmetry in plans, We first compare the story drifts of mass centers in the first stories of the buildings with various mass eccentricities. The result of such a comparison is the percentage of increase in drifts of the first stories mass center with increasing

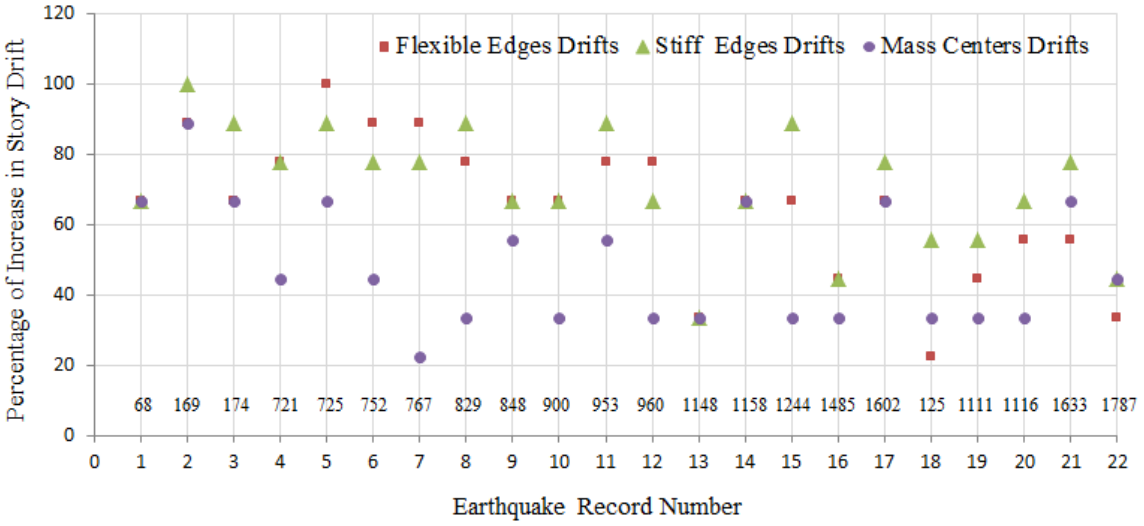

Fig. 8 The percentage of increase in story drift in mass centers, stiff and flexible edges with increase in the mass eccentricity

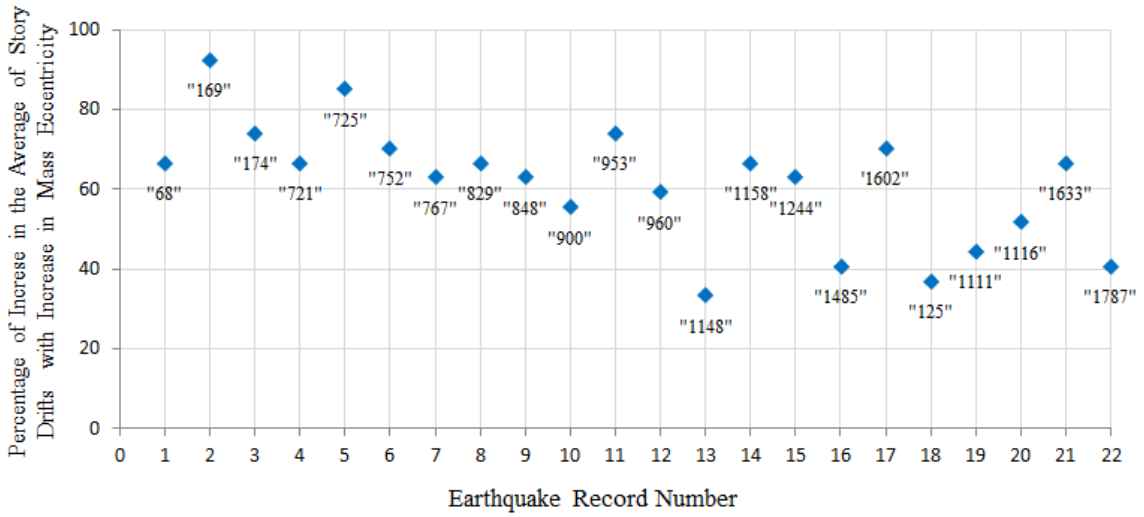

Fig. 9 The percentage of increase in the average of story drifts in mass centers, stiff and flexible edges with increase in the mass eccentricity

of mass eccentricity. This procedure is repeated for both of stories 2 and 3. Averaging over 3 drift values relevant to stories 1, 2 and 3, yields the percentage of increase in story drifts of the mass centers for the entire buildings. This method is repeated for the stiff and flexible edges, and the percentages of increase in the story drifts at mass centers, stiff and flexible edges are calculated separately. Results are shown in Fig. 8. Finally, averaging over drifts of mass center, stiff and flexible edges, yields the percentage of increase in the story drift of the entire buildings with increasing the mass eccentricities in plan. Results are shown in Fig. 9.

Back to Fig. 8, with increasing the mass eccentricity, the percentages of increase in the story

drifts of mass center are less than those in stiff and flexible edges. This figure also shows that the trend in the stiff edge is relatively similar to that of flexible edge.

Combining the data of Figs. 7 and 8, produces Fig. 10. As this figure shows, with increasing the mass eccentricity, the percentages of increase in the number of collapsed hinges in the whole of the buildings are closer to the percentages of increase in drifts of the mass centers, and consequently they are less than the percentages of increase in drifts of stiff and flexible edges. In other words, in majority of the earthquake records (almost 77%), the percentages of increment in the number of collapsed hinges are closer to the percentages of increment in the mass centers in comparison with those of the stiff and flexible edges. Also there is a similar trend between the number of collapsed hinges and the story drifts of the mass centers which are shown with the thin lines in Fig. 10.

Combining the data on Figs. 7 and 9, produces Fig. 11. As this figure shows, when the mass eccentricity increases, the percentages of increase in the number of collapsed hinges in the whole

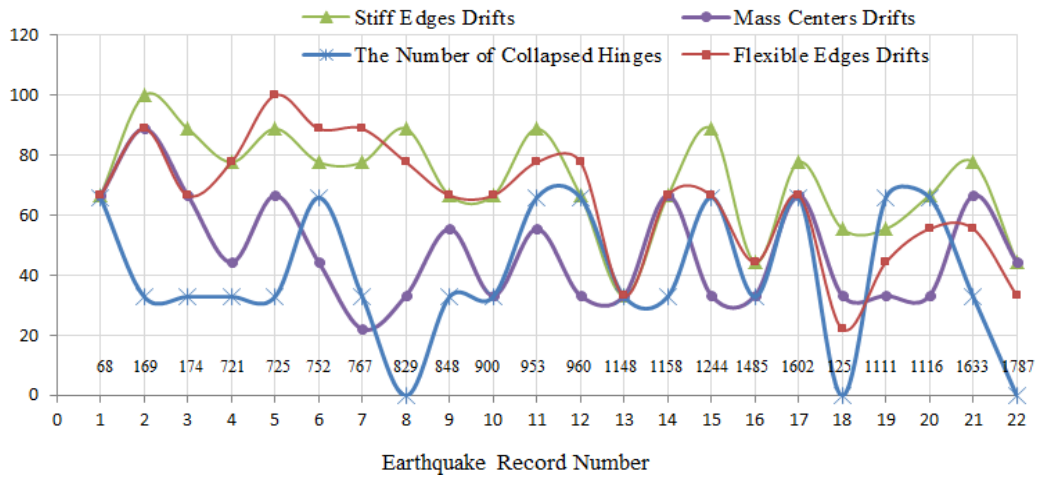

Fig. 10 The percentage of the number of collapsed hinges and story drifts increase in the mass centers, stiff and flexible edges with increase in the mass eccentricity in plan

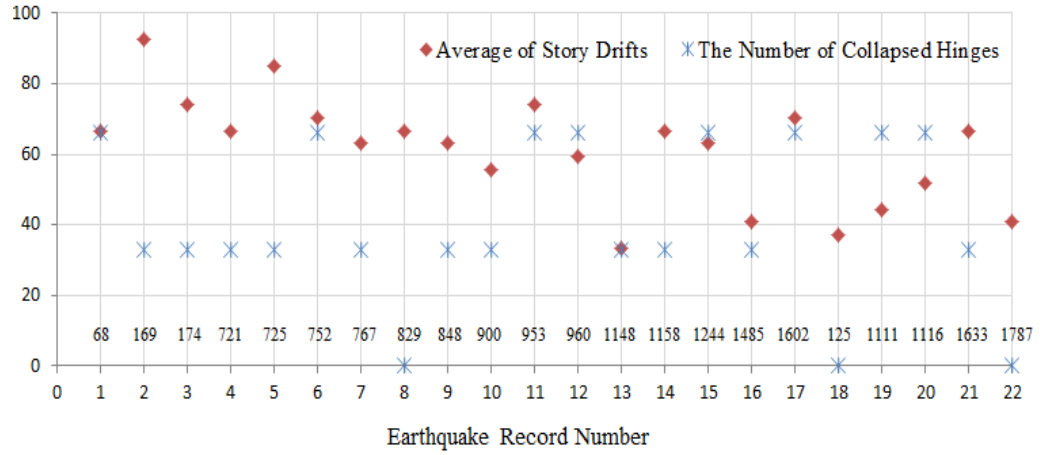

Fig. 11 The percentage of increase in the number of collapsed hinges and the average of story drifts with the mass eccentricity increase in buildings

of buildings is less than the percentages of increase in the average story drifts of the mass centers, stiff and flexible edges.

According to Figs. 10 and 11, we conclude that there are two relationships between the number of collapsed hinges and the value of story drifts in the mass center, stiff and flexible edges. First, with increasing the mass eccentricity, the percentages of increase in the number of collapsed hinges are closer to the percentage of increase in the story drifts in the mass centers. Moreover with increasing the mass eccentricity, the percentage of increase in the number of collapsed hinges, are less than the percentages of increase in the average story drifts of the mass centers, stiff and flexible edges.

It is worth mentioning that these two observations are not conflicting and are compatible. Therefore, the percentages of increase in the number of collapsed hinges are not only closer to the story drifts of the mass centers but also are less than the percentages of increase in the average story drifts of the mass centers, stiff and flexible edges.

The drifts which have shown in Fig. 11 are the average of the story drifts shown in Fig. 10. So, Figs. 10 and 11 are not inconsistent.

These indicate that to have a more accurate estimation of the number of collapse hinges, we can use both of the observations.

3. Conclusions

- Progressive collapse assessment of a 3-story symmetric reinforced concrete ordinary moment resisting frame building in comparison with the asymmetric buildings shows that the building behavior with respect to the number of collapsed beam and column hinges is similar to the trend of the story drifts at the mass centers.
- With increase of mass eccentricity, the increase of drift in the stiff edge is relatively similar to that of the flexible edge and both are greater than the increase of mass center.
- With increasing the mass eccentricity from 0% to 25%, the potential of progressive collapse increases around 41% in average.

References

Alashker, Y., Li, H. and EL-Tawil, S. (2011), "Approximations in progressive collapse modeling", *J. Struct. Eng.*, **137**, 914-924.

Burnett, E.F.P. (1975a), "Abnormal loading and building safety", American Concrete Institute, *Int. Concrete Res.Inform. Portal*, SP **48**, 141-190.

Bažant, Zdenfk P. and Verdure, Mathieu (2007), "Mechanics of progressive collapse: learning from world trade center and building demolitions", *Eng. Mech.*, **133**(3).

Biskinis, D. and Fardis, M.N. (2009), "Deformations of concrete members at yielding and ultimate under monotonic or cyclic loading (including repaired and retrofitted members)", Report Series in Structural and Earthquake Engineering, Report No. SEE 2009-01.

Bao, Yihai., Kunnath, Sashi K., El-Tawil ,Sherif and Lew, H.S. (2012), "Macromodel-based simulation of progressive collapse: RC frame structures", *Struct. Eng.*, **134**(7), 1079-1091.

Dides, M.A. and Llera, J.C. (2005), "A comparative study of concentrated plasticity models in dynamic analysis of building structures", *J. Earthq. Eng. Struct. Dyn.*, **34**(8), 1005-1026.

Ellingwood, B. (2006), "Mitigating risk from abnormal loads and progressive collapse", *J. Perform. Constr.*

Facil., **20**, SPECIAL ISSUE: Mitigating the Potential for Progressive Disproportionate Structural Collapse, 315-323.

El-Tawil, S., Khandelwal, K., Kunnath, S., Lew. H.S. (2007), "Macro models for progressive collapse analysis of steel moment frame buildings", *Proc. Structures Congress 2007*, Long Beach, CA.

Ettouney, Mohammed, Smilowitz, Robert, Tang, Margaret and Hapij, Adam (2012), "Global system considerations for progressive collapse with extensions to other natural and man-made hazards", *J. Perform. Constr. Facil.*, **20**, SPECIAL ISSUE: Mitigating the Potential for Progressive Disproportionate Structural Collapse, 403-417.

Eslami, A. and Ronagh, H.R. (2012), "Effect of elaborate plastic hinge definition on the pushover analysis of reinforced concrete buildings. Struct", *J. Des. Tall Spec. Build*., doi: 10.1002/tal.1035.

FEMA P695 (2009), *Quantification of building seismic performance factors*, Prepared by Applied Technology Council, www.ATCouncil.org.

Filippou, F.C. (1999), "Analysis platform and member models for performance-based earthquake engineering", U.S.-Japan Workshop on Performance-Based Earthquake Engineering Methodology for Reinforced Concrete Building Structures, PEER Report 1999/10, Pacific Earthquake Engineering Research Center, University of California, Berkeley, California, pp. 95-106.

Gurley, C. (2012), "Progressive collapse and earthquake resistance", *Pract. Period. Struct. Des. Constr-ASCE*, **13**(1), 19-23.

Haselton, C.B. and Deierlein, G.G. (2007), "Assessment seismic collapse safety of modern reinforced concrete moment frame building", The John A. Blume Earthquake Engineering Center, Stanford University.

Haselton, C.B., Liel, A.B., Lange, S.T. and Deierlein, G.G. (2008), "Beam-column element model calibrated for predicting flexural response leading to global collapse of RC frame buildings", PEER Report 2007/03, Pacific Earthquake Engineering Research Center, College of Engineering University of California, Berkeley.

Haselton, C.B., Liel, A.B. and Deierlein, G.G. (2008), "Simulating structural collapse due to earthquakes: model idealization, model calibration, and numerical solution algorithms", *COMPDYN2009 ,ECCOMAS Thematic Conference on Computational Methods in Structural Dynamics and Earthquake Engineering*, Greece.

Helmy, Huda, Salem, Hamed, Mourad, Sherif (2012), "Progressive collapse assessment of framed reinforced concrete structures according to UFC guidelines for alternative path method", *Eng. Struct.*, **42**, 127-141.

Hayes, Jr., John, R., Woodson, Stanley C., Pekelnicky, Robert G., Poland, Chris D., Corley, W. Gene and Sozen, Mete (2012), "Can strengthening for earthquake improve blast and progressive collapse resistance?", *Struct. Eng.- ASCE*, **131**(8), 1157-1177.

Ibarra, L.F. and Krawinkler, H. (2004), "Global collapse of deteriorating MDOF systems", *Proc.13thWorld Conference on Earthquake Engineering*, Vancouver, B.C., Canada, August 1-6, Paper No. 116.

Ibarra, L.F. (2005), "Global collapse of frame structures under seismic excitations", Ph.D. thesis, Stanford Univ.

Ibarra, L.F., Medina, R.A. and Krawinkler, H. (2005), "Hysteretic models that incorporate strength and stiffness deterioration", *J. Earthq. Eng. Struct. Dyn.*, **34**, 1489-1511.

Kaewkulchai, Griengsak and Williamson, Eric B. (2003), "Beam element formulation and solution procedure for dynamic progressive collapse analysis", *Comput. Struct.*, **82**(7-8), 639-651.

Kyakula, M. and Wilkinson, S. (2004), "Analyses of R/C frames subjected to seismic loading", *13th World Conference on Earthquake Engineering*, Vancouver, B.C., Canada, Paper No. 933.

Khandelwala, Kapil, El-Tawila, Sherif, Sadekb, Fahim (2009), "Progressive collapse analysis of seismically designed steel braced frames", *Constr. Steel Res.*, **65**(3), 699-708.

Krawinkler, H., Zareian, F., Lignos, D.G. and Ibarra, L.F. (2009), "Prediction of collapse of structures under earthquake excitations", *COMPDYN 2009, ECCOMAS Thematic Conference on Computational Methods in Structural Dynamics and Earthquake Engineering*, Greece.

Kim, J. and Hong, S. (2011), "Progressive collapse performance of irregular buildings", *J. Struct. Des. Tall Sp. Build.*, **20** (6), 721-734.

Kim, J., Choi, H., Min, K.W. (2011), "Use of rotational friction dampers to enhance seismic and progressive collapse resisting capacity of structures", *J. Struct. Des. Tall Sp. Build.*, **20**(4), 515-537.
Khandelwal, K., El-Tawil, S., Kunnath, S. and Lew, H.S. (2012), "Macromodel-based simulation of progressive collapse: steel frame structures", *Struct. Eng.*, **134**(7), 1070-1078.
Lew, H.S. (2003), *Best practices guidelines for mitigation of building progressive collapse*, National Institute of Standards and Technology, Gaithersburg, Maryland, U.S.A, 20899-8611, hsl@nist.gov.
Lignos, D.G. (2008), "Sidesway collapse of deteriorating structural systems under seismic excitations", Ph.D. Thesis, Stanford Univ.
Lignos, D.G., Zareian, F. and Krawinkler, H. (2008), "Reliability of a 4-story steel moment-resisting frame against collapse due to seismic excitations", *ASCE Structures Congress*, pp. 1-10.
Lu, X.Z., Lin, X., Ma, Y., Li, Y. and Ye, L. (2008), "Numerical simulation for the progressive collapse of concrete building due to earthquake", *Proc. the 14th World Conference on Earthquake Engineering*, Beijing, China.
Lu, X.Z., Li, Y., Ye, L.P., Ma, Y.F. and Liang, Y. (2008), "Study on the design methods to resist progressive collapse for building structures", *Proc.Tenth Int. Symp. On Structural Engineering for Young Experts*., Oct. 2008, Changsha,478-483.
Lignos, D. and Krawinkler, H. (2012), "Development and utilization of structural component databases for performance-based earthquake engineering", *J. Struct. Eng*., 10.1061/(ASCE) ST.1943-541X.0000646 (Aug. 10, 2012).
Masoero, E., Wittel, F., Herrmann, H. and Chiaia, B. (2010), "Progressive collapse mechanisms of brittle and ductile framed structures", *J. Eng. Mech*., **136**(8), 987-995.
Pekau, O.A. and Cui, Yuzhu (2005), "Progressive collapse simulation of precast panel shear walls during earthquakes", *Comput. Struct.*, **84(**5-6), 400-412.
Panagiotakos, T.B. and Fardis, M.N. (2009),"Deformations of rinforced cncrete mmbers at yelding and utimate", *Struct. J.*, **98**(2), 135-148.
Sasani, M., Bazan, M. and Sagiroglu, S. (2007), "Experimental and analytical progressive collapse evaluation of an actual RC structure", *Struct. J.*, **104**(6), 731-739.
Sasani, M. and Kropelnicki, J. (2008), "Progressive collapse analysis of an RC structure", *Struct. Design Tall Spec. Build.*, **17**(4), 757-771.
Sasani, M. and Sagiroglu, S. (2008), "Progressive collapse resistance of hotel San Diego", *J. Struct. Eng.*, **134(**3), 478-488.
Sasani, M. and Sagiroglu, S. (2008), "Progressive collapse of RC structures: a multihazard perspective", *Struct. J.*, **105(**1), 96-103.
Somes, N.F. (1973), "Abnormal loading on buildings and progressive collapse", in Building Practices for Disaster Mitigation (Wright, Kramer and Culver, eds.), Building Science Series No. 46, National Bureau of Standards, Washington, DC.
Tsai, Meng-Hao and Lin, Bing-Hui (2008), "Investigation of progressive collapse resistance and inelastic response for an earthquake-resistant RC building subjected to column failure", *J. Eng. Struct.*, **30(**12), 3619-3628.
Talaat, M. and Mosalam, K.M. (2009), "Modeling progressive collapse in reinforced concrete buildings using direct element removal", *Earthq. Eng. Struct. Dyn*., **38**, 609-634.
Yi, L.I., Lu, Xin-Zheng and Ye, Lie-Ping (2011), "Study on the progressive collapse mechanism of RC frame structures", *Build. Sci.*, **27**(5), 12-18.
Zareian, F., Lignos D.G. and Krawinkler, H. (2009), "Quantification of modeling uncertainties for collapse assessment of structural systems under seismic excitations", *COMPDYN 2009, ECCOMAS Thematic Conference on, Computational Methods in Structural Dynamics and Earthquake Engineering*, Greece.
Zareian, F. and Medina, R.A. (2010), "A practical method for proper modeling of structural damping in inelastic plane structural systems", *Comput.Struct.*, **88**, 45-53.

Appendix: the list of notations

δc = cap deformation (deformation associated with Fc for monotonic loading)
Fy = effective yield strength, incorporating "average" strain hardening
δy = effective yield deformation (= Fy/Ke)
Ke = effective elastic stiffness
Fr = residual strength capacity
δr = deformation at residual strength
δu = ultimate deformation capacity
δp = plastic deformation capacity associated with monotonic loading
δpc = post-capping deformation capacity associated with monotonic loading
Fc/Fy = post-yield strength ratio
Fyp = predicted effective yield strength (predicted from measured material properties)
Fyn = nominal effective yield strength (predicted from nominal material properties)
κ = residual strength ratio = Fr/Fy
Strain hardening ratio $\alpha s = Ks/Ke = [(Fc/Fy)/\delta p]/Ke$
Post-capping stiffness ratio $\alpha c = Kpc/Ke = (Fc/\delta pc)/Ke$
Fc = strength cap (maximum strength, incorporating "average" strain hardening)
My = yield moment for Ibarra material model (nominal moment capacity of the column)
Mc = moment capacity at the capping point; used for prediction of hardening stiffness
Kc = post-capping stiffness, i.e., stiffness beyond $\Theta cap, pl$
Ke = effective elastic secant stiffness to the yield point
Ks = hardening stiffness, i.e., stiffness between Θy and $\Theta cap, pl$
Θy = chord rotation at yielding, taken as the sum of flexural, shear and bond-slip components; yielding is defined as the point of significant stiffness change, i.e., steel yielding or concrete crushing (radians)
Θcap = θcap^{tot} = total chord rotation at capping, sum of elastic and plastic deformations (radians)
θcap^{p} (Or Θp) = plastic chord rotation from yield to cap (radians)
Θp = plastic chord rotation from yield to cap (radians)
Θpc = post-capping plastic rotation capacity, from the cap to point of zero strength (radians)
$\Theta u = \Theta y + \Theta p + \Theta pc$